Supporting Information

Improved High-Current-Density Hydrogen Evolution Reaction Kinetics on Single-Atom Co Supported on Ordered Nitrogen Assembly Carbon Support

Jiaqi Yu[a]†, Yu Yan[b]†, Yuemin Lin[a,f]†, Hengzhou Liu[c], Yuting Li[d], Shaohua Xie[e], Simin Sun[a], Fudong Liu[e], Zhiguo Zhang[f], Wenzhen Li[c], Jin-Su Oh[d], Lin Zhou[d], Long Qi[d], Bin Wang[b]*, Wenyu Huang[a,d]**

[a.] *Department of Chemistry, Iowa State University, Ames, IA 50011 USA. E-mail: whuang@iastate.edu*
[b.] *School of Chemical, Biological and Materials Engineering, University of Oklahoma, Norman, OK, 73019 USA. E-mail: wang_cbme@ou.edu*
[c.] *Department of Chemical and Biological Engineering, Iowa State University, Ames, IA 50011, USA*
[d.] *U.S. DOE Ames National Laboratory, Iowa State University, Ames, IA 50011, USA. E-mail: lqi@iastate.edu*
[e.] *Department of Chemical and Environmental Engineering, University of California, Riverside, CA 92521, United States*
[f.] *Key Laboratory of Biomass Chemical Engineering of Ministry of Education, College of Chemical and Biological Engineering, Zhejiang University, Hangzhou 310058, P.R. China*
† These authors contributed equally to this work.

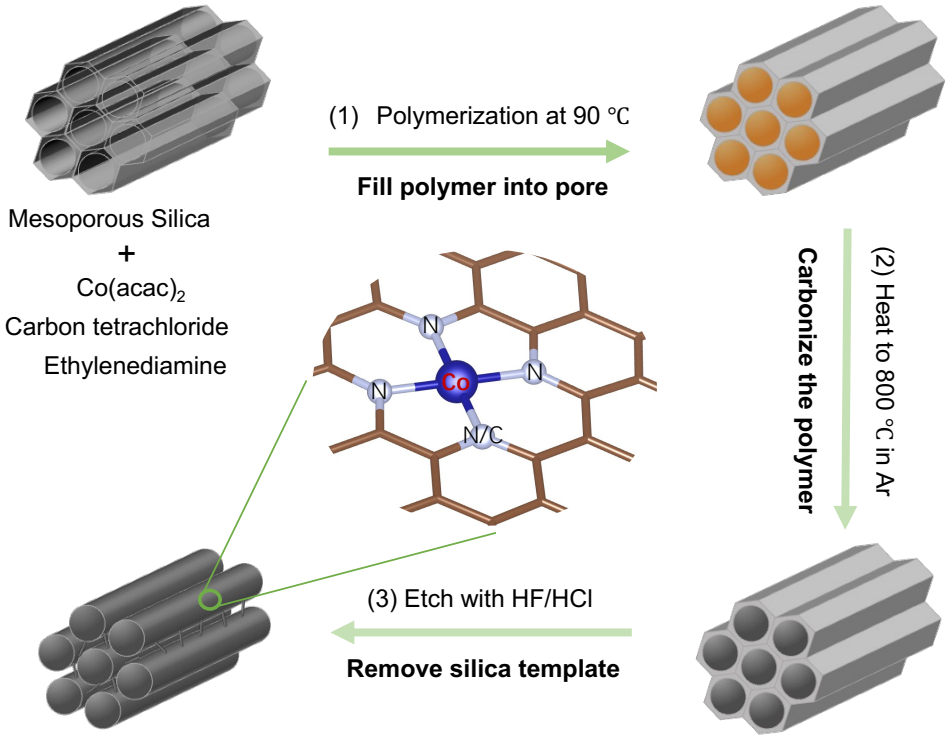

Scheme S1. Synthesis procedure for single-atom Co-NAC with aligned pore structure using mesoporous silica template.

Table S1. ICP-MS characterizations of Co loading on different Co-NAC catalysts.

Catalyst	**Co loading**
Co-100-NAC-600	1.2 wt.%
Co-100-NAC-700	1.7 wt.%
Co-100-NAC-800	1.9 wt.%
Co-50-NAC-800	1.1 wt.%
Co-25-NAC-800	0.6 wt.%

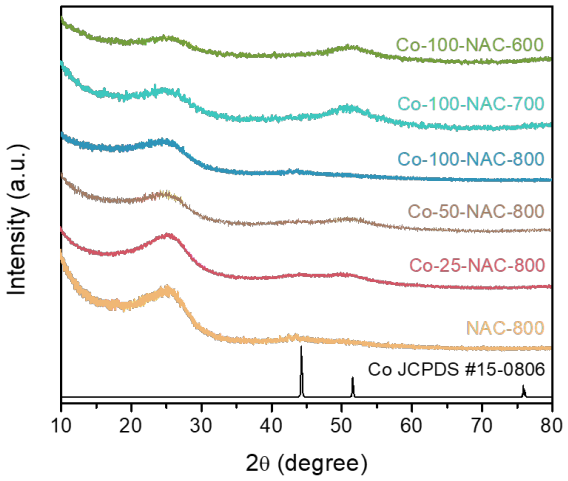

Figure S1. PXRD patterns of Co-NAC catalysts prepared under different conditions.

Table S2. N_2-sorption characterization of NAC catalysts.

Sample	Surface area[a] ($m^2\ g^{-1}$)	Average pore diameter[b] (nm)	Pore volume ($cm^3\ g^{-1}$)
Co-100-NAC-600	570	3.6	0.48
Co-100-NAC-700	770	3.7	0.73
Co-100-NAC-800	1256	3.7	1.12
Co-50-NAC-800	689	3.8	0.68
Co-25-NAC-800	727	3.8	0.70
NAC-800	696	3.5	0.61

[a] BET surface area.
[b] BJH average pore diameter obtained from the desorption branch.

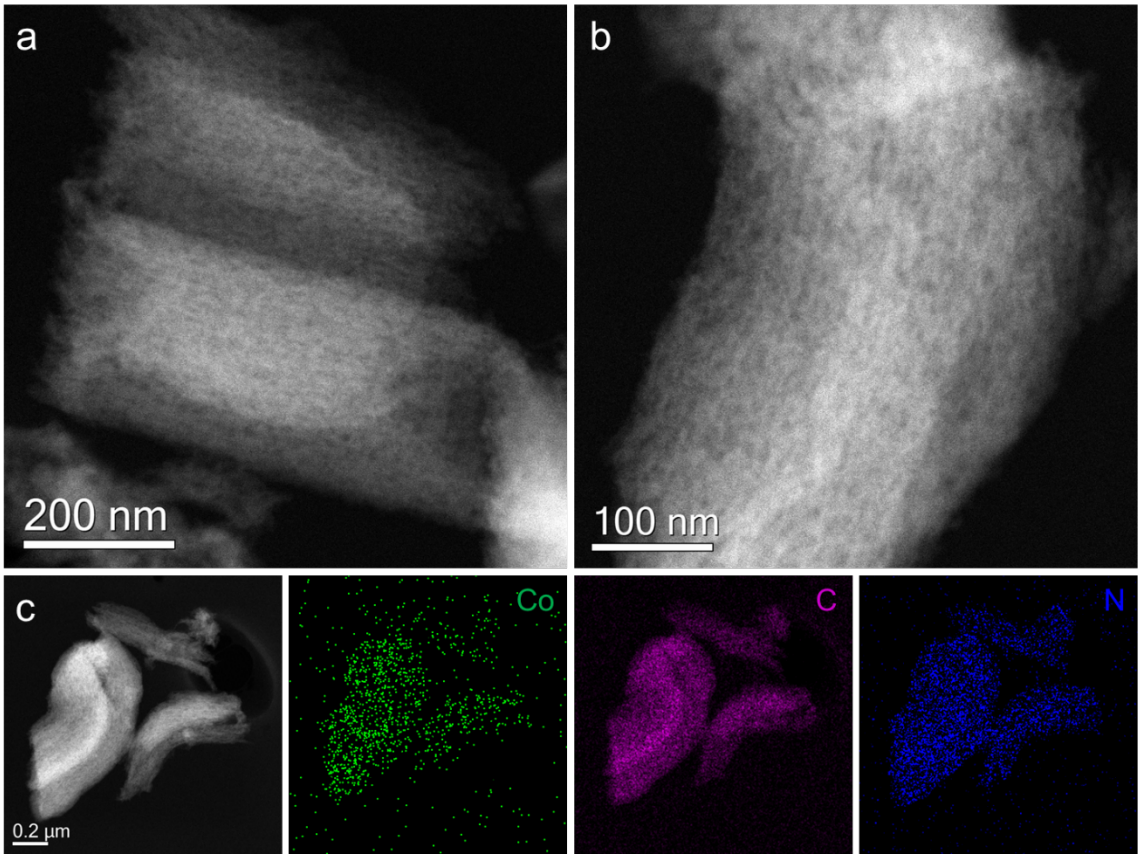

Figure S2. STEM and EDS mapping images of the as-synthesized Co-100-NAC-800. (a,b) STEM images showing order pore structure; (c) EDS mapping images showing the uniform distribution of Co, N, and C.

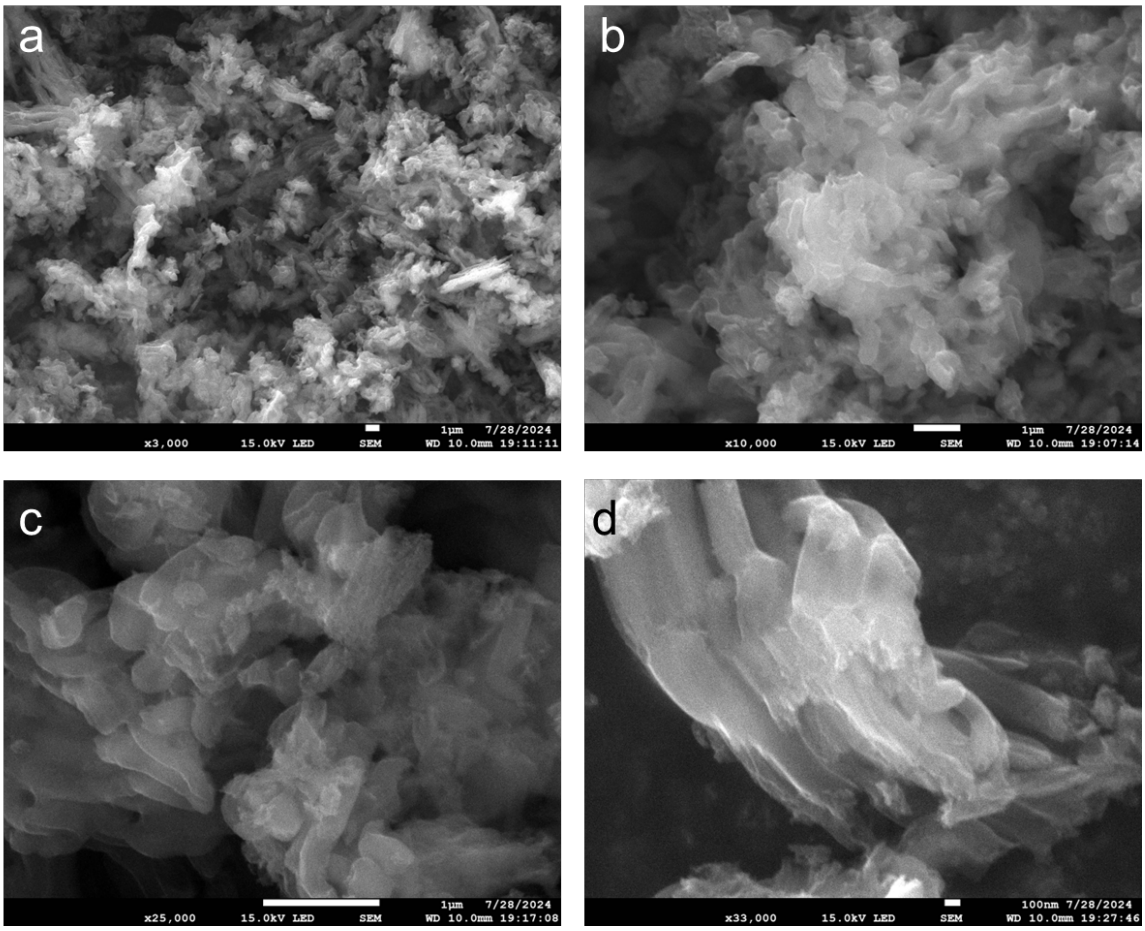

Figure S3. SEM images of synthesized Co-100-NAC-800 at different magnifications.

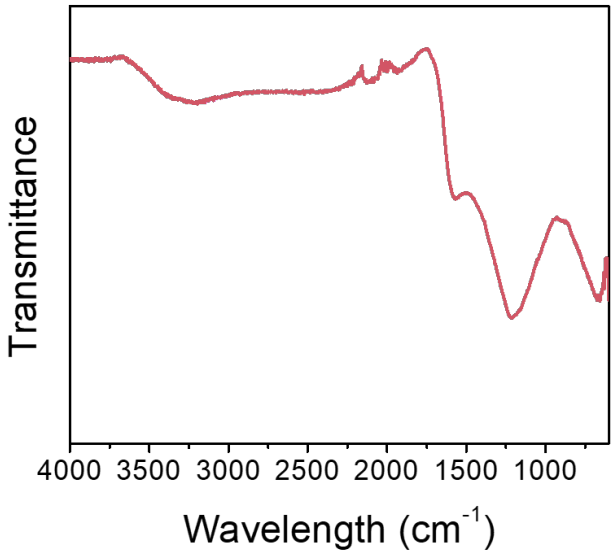

Figure S4. Attenuated Total Reflectance Fourier Transform Infrared Spectroscopy (ATR-FTIR) spectrum of synthesized Co-100-NAC-800.

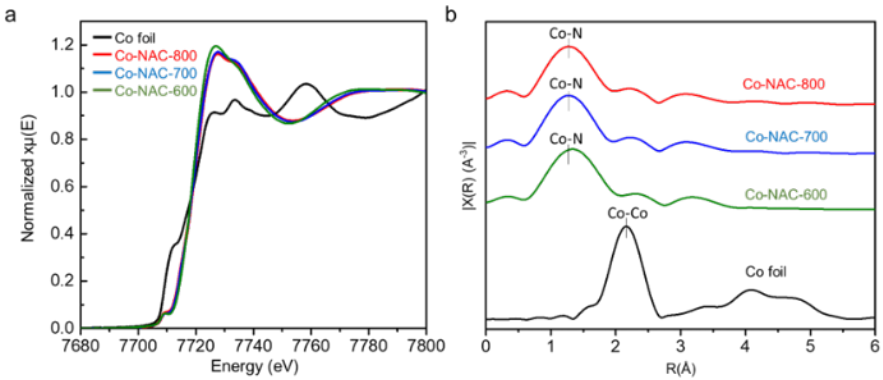

Figure S5. XANES and EXAFS spectra of single-atom Co catalyst. (a) Energy space of Co K-edge of single-atom Co catalysts carbonized under Ar at different temperatures ranging from 600 to 800 °C; (b) R-space of Co K-edge of single-atom Co catalysts. The XAS data of Co-NAC-800 had been published in our previous work and added here for comparison purposes.[1]

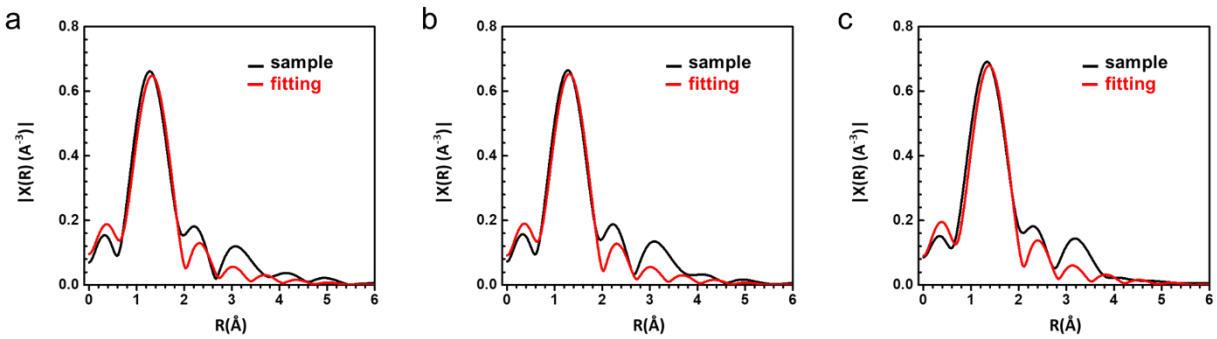

Figure S6. EXAFS spectra of (a) Co-100-NAC-800; (b) Co-100-NAC-700; (c) Co-100-NAC-600. The data of Co-NAC-800 had been published in our previous work and added here for comparison purposes.[1]

Table S3. EXAFS fitting parameters for Co catalysts (k-range = 2.5 to 8.5 Å^{-1})

Sample	**Shell**	**CN**[a]	**R (Å)**[b]	**σ^2 (Å^2)**[c]
Co-100-NAC-800[e]	Co-N	4[d]	1.94 ± 0.03	0.006 ± 0.002
Co-100-NAC-700	Co-N	4[d]	1.94 ± 0.03	0.007 ± 0.002
Co-100-NAC-600	Co-N	4[d]	1.99 ± 0.03	0.005 ± 0.002

[a] Coordination number; [b] Bond length; [c] Debye-Waller factor; [d] The coordination number of Co-NAC samples is fixed. [e] The data of Co-NAC-800 had been published in our previous work and added here for comparison purposes.[1]

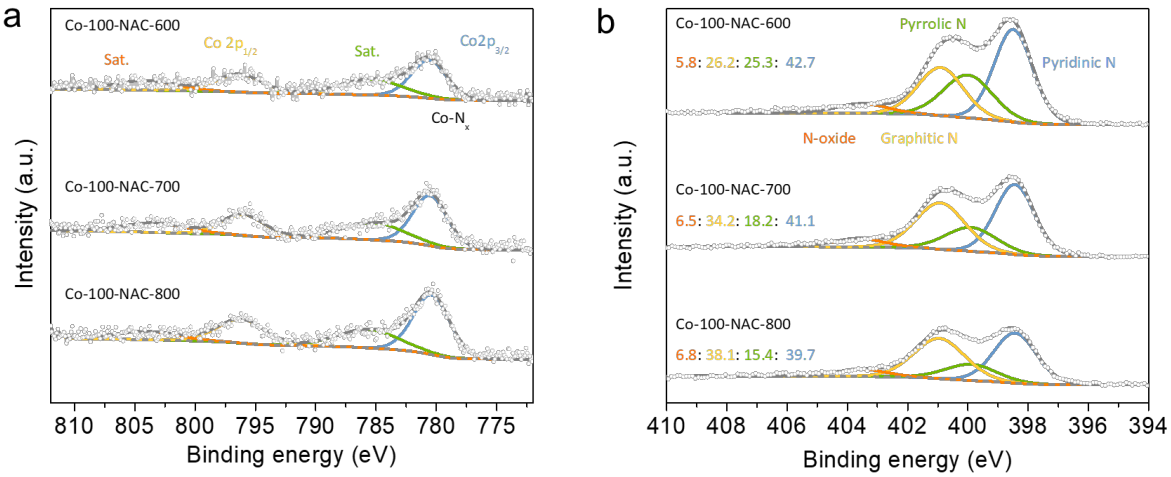

Figure S7. XPS of Co-NAC prepared at different temperatures. (a) Co2p Spectre and (b) N1s Spectre.

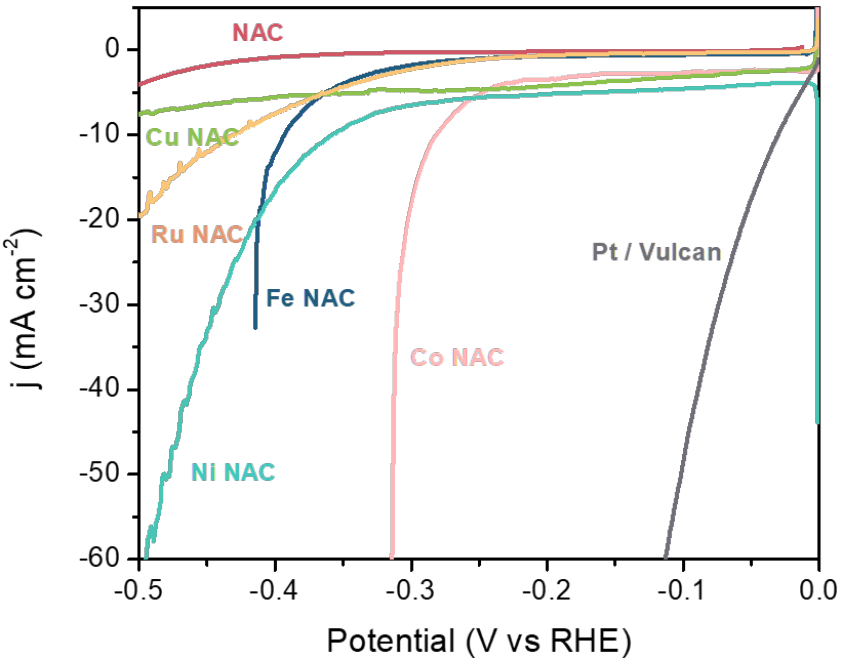

Figure S8. LSV of different transition metal single-atom on NAC for HER. 1 M KOH as electrolyte, M-NAC on carbon fiber paper as working electrode, Pt as counter electrode, Ag/AgCl as reference electrode. A Nafion membrane separates working and counter electrodes.

Table S4. CHNS analysis of Co-NAC pyrolyzed at different temperatures.

Catalyst	N (wt.%)	C (wt.%)	H (wt.%)
Co-100-NAC-600	19.94	64.15	2.76
Co-100-NAC-700	17.34	66.76	2.30
Co-100-NAC-800	13.15	69.14	2.10

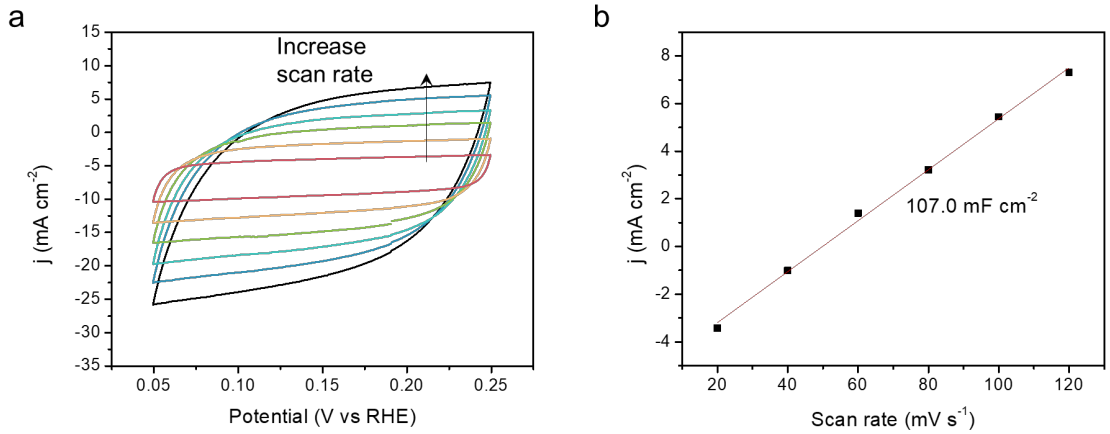

Figure S9. ECSA estimation of Co-25-NAC-800. (a) CV curve at potential range 0.05-0.25 V vs RHE; (b) linear relationship between current density and scan rate.

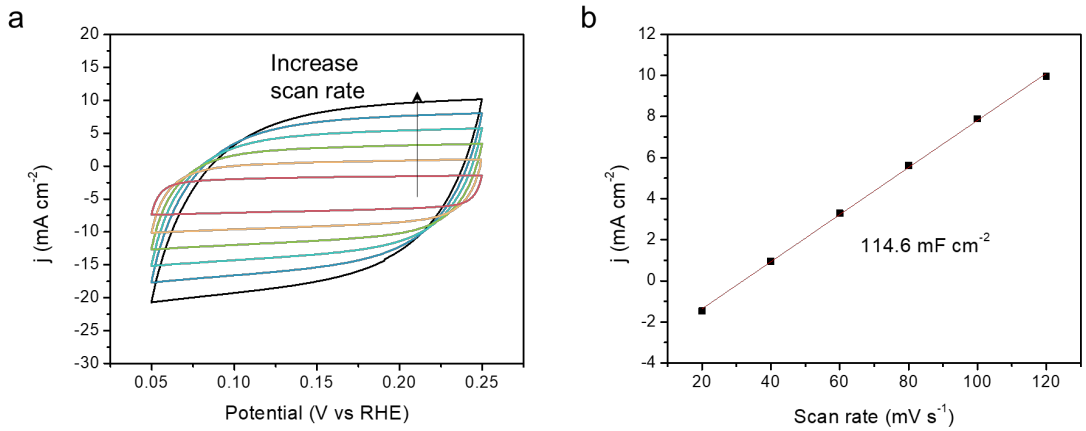

Figure S10. ECSA estimation of Co-50-NAC-800. (a) CV curve at potential range 0.05-0.25 V vs RHE; (b) linear relationship between current density and scan rate.

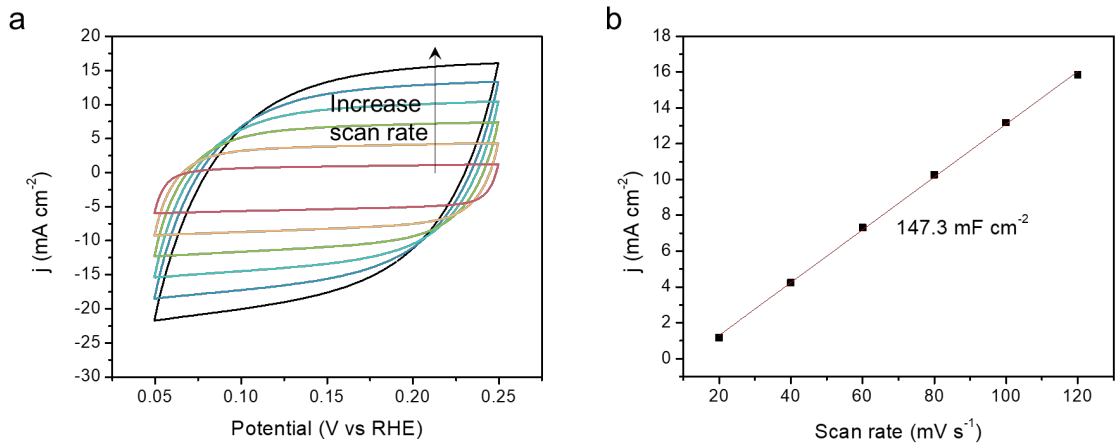

Figure S11. ECSA estimation of Co-100-NAC-800. (a) CV curve at potential range 0.05-0.25 V vs RHE; (b) linear relationship between current density and scan rate.

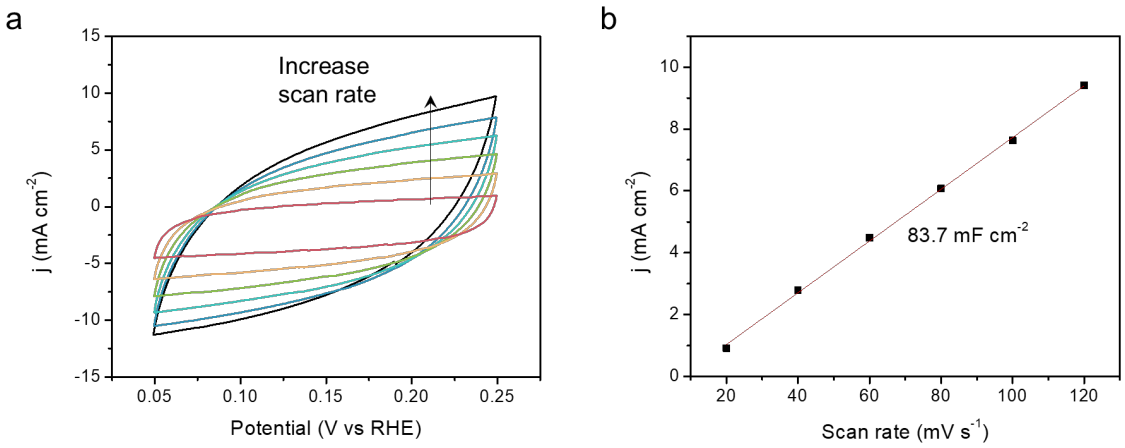

Figure S12. ECSA estimation of NAC-800. (a) CV curve at potential range 0.05-0.25 V vs RHE; (b) linear relationship between current density and scan rate.

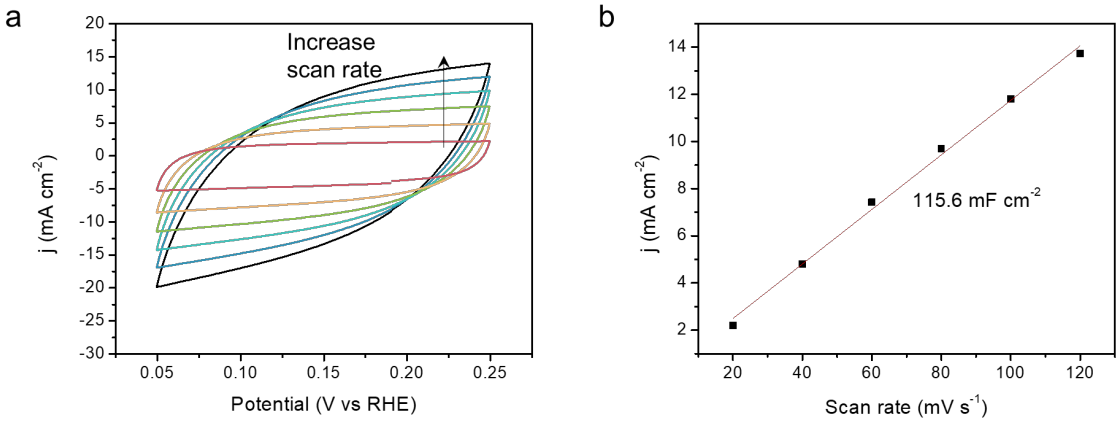

Figure S13. ECSA estimation of Co-100-NAC-700. (a) CV curve at potential range 0.05-0.25 V vs RHE; (b) linear relationship between current density and scan rate.

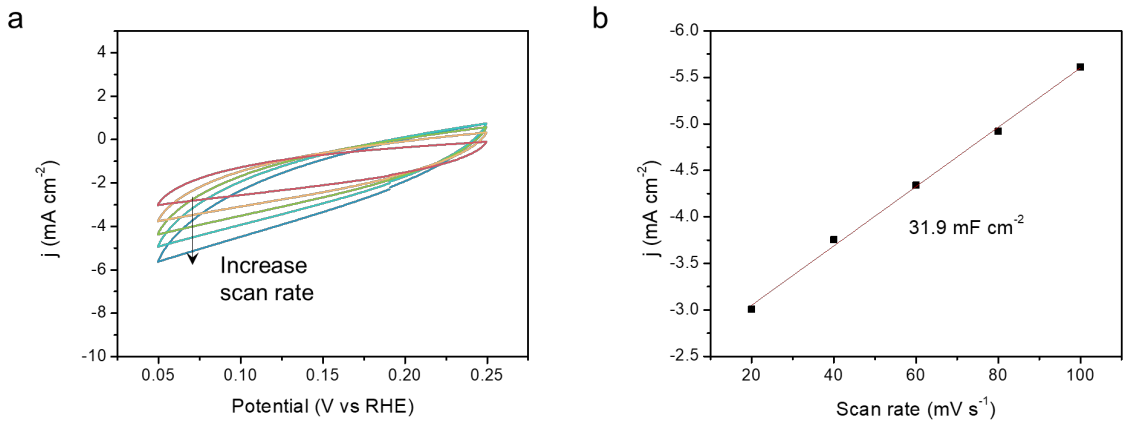

Figure S14. ECSA estimation of Co-100-NAC-600. (a) CV curve at potential range 0.05-0.25 V vs RHE; (b) linear relationship between current density and scan rate.

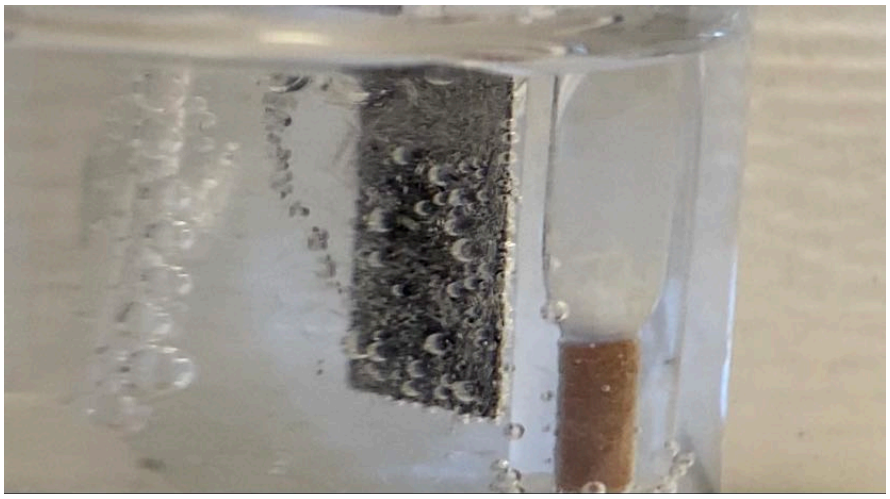

Figure S15. Photo showing hydrogen production during the stability test.

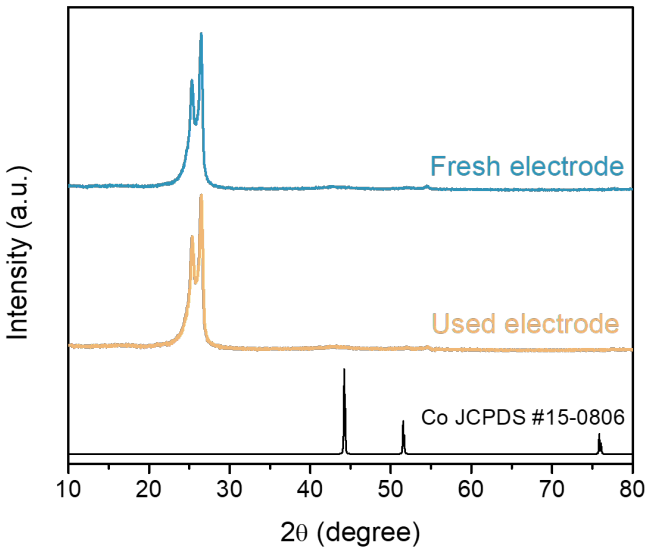

Figure S16. XRD characterization of the Co-100-NAC-800 electrode before and after HER test. Blue line: fresh Co-100-NAC-800 electrode; orange line: Co-100-NAC-800 after 20 h stability test. No diffraction pattern change or Co aggregation was observed.

Table S5. The bond length between the metal and the substrate atom calculated from different Co-NAC configurations. The table shows the average value of the bond length.

Metal Bond with substrate (Å)	**CoN_1**	**Ortho-CoN_2**	**Meta-CoN_2**	**CoN_3**	**CoN_4**
Co-N	1.93	1.91	1.90	1.89	1.88
Co-C	1.88	1.87	1.88	1.84	/

Table S6. Comparison of the HER reaction activity between our catalyst and other reported Co-based catalysts.

Catalyst	**Overpotential (mV @ mA/cm^2)**	**Electrolyte**	**Reference**
Co-100-NAC-800	310@200	1 M KOH	This work
$CoSe_2/Co_3S_4@Co_3O_4$	165@10 393@ 200	1 M KOH	2
Co/SmH_2	252@100	1.0 M KOH	3
$CoPS_3$ /CoS_2 heterojunction	36.3@10	0.5 M H_2SO_4	4
$Ti/Na_2Ti_6O_{13}/Co(OH)_2$	159 @10	1.0 M KOH	5
CoP/Co_2P-H	97@10	1.0 M KOH	6
$CoP\text{-}Co_xO_y$/CC	43@10	1.0 M KOH	7
Co_3O_4/MXene	118@10	1.0 M KOH	8
Co/Co_xS_y@NC-750	330@10	1.0 M KOH	9
$NbSSe\text{-}Co_{0.1}$	173@10	0.5 M H_2SO_4	10
2D CoP	144@10	1.0 M KOH	11
VO_x-doped CoP	65@10 245@400	1.0 M KOH	12
$Co/CoO/B_2O_3$/CF	16@10 100@100	1.0 M KOH	13
Ni_2P/CoP/NF	56@30 118@100	1.0 M KOH	14
$Ni_{0.67}Co_{0.33}/Ni_3S_2$@NF	87@10 203@100	1.0 M KOH	15
Co/N−CNF	241@10	1.0 M KOH	16
Co@Zn-N-CNTs	67@10	0.5 M H_2SO_4	17

Reference:

1. Y. Lin, R. Nie, Y. Li, X. Wu, J. Yu, S. Xie, Y. Shen, S. Mao, Y. Chen, D. Lu, Z. Bao, Q. Yang, Q. Ren, Y. Yang, F. Liu, L. Qi, W. Huang and Z. Zhang, *Nano Res.*, 2022, **15**, 10006-10013.
2. C. Sun, C. Wang, H. Xie, G. Han, Y. Zhang and H. Zhao, *Small*, 2023, **19**, 2302056.
3. Z. Chen, S. Mebs, I. Mondal, H. Yang, H. Dau, Z. Kang, M. Haumann, S. Ghosh, W. Cen, M. Driess and P. W. Menezes, *Advanced Functional Materials*, **n/a**, 2402699.
4. K. Song, H. Zhang, Z. Lin, Z. Wang, L. Zhang, X. Shi, S. Shen, S. Chen and W. Zhong, *Advanced Functional Materials*, 2024, **34**, 2312672.
5. M. Amiri, J. Dondapati, J. Quintal and A. Chen, *ACS Appl. Mater. Interfaces*, 2022, **14**, 40021-40030.
6. X. Cao, J. Tian, Y. Tan, Y. Zhu, J. Hu, Y. Wang, E. Liu and Z. Chen, *Small*, 2024, **20**, 2306113.
7. M. M. Alsabban, M. K. Eswaran, K. Peramaiah, W. Wahyudi, X. Yang, V. Ramalingam, M. N. Hedhili, X. Miao, U. Schwingenschlögl, L.-J. Li, V. Tung and K.-W. Huang, *ACS Nano*, 2022, **16**, 3906-3916.
8. M. Ghaemmaghami and Y. Yamini, *ACS Appl. Mater. Interfaces*, 2024, **16**, 18782-18789.
9. H. D. Mai, P. M. Park, G.-N. Bae, S. Jeong, B. Seo, M. Cho, S. Park, N. D. Cuong, T. V. Cuong, N. M. Tran, C.-M. Park and K.-J. Jeon, *J. Mater. Chem. A*, 2024, **12**, 4761-4769.
10. Y. Ren, X. Miao, J. Zhang, Q. Lu, Y. Chen, H. Fan, F. Teng, H. Zhai, X. He, Y. Long, C. Zhang and P. Hu, *J. Mater. Chem. A*, 2023, **11**, 2690-2697.
11. X. Guo, M. Duan, J. Zhang, B. Xi, M. Li, R. Yin, X. Zheng, Y. Liu, F. Cao, X. An and S. Xiong, *Advanced Functional Materials*, 2022, **32**, 2209397.
12. R. Li, P. Ren, P. Yang, Y. Li, D. Wang, X. Lu, H. Zhang, F. Meng, X. Peng, B. Yuan, B. Wang, J. Zhang, M. An and G. Wu, *Nano Energy*, 2024, **126**, 109613.
13. Y. Ren, J. Wang, W. Wang, H. Wen, M. Chen, Y. Qiu, G. Li, Z. Yang and P. Wang, *J. Mater. Chem. A*, 2023, **11**, 13282-13288.
14. S. Niu, J. Wang, Y. Wu, J. Zhang, X. Wu, H. Luo and W.-J. Jiang, *ACS Appl. Mater. Interfaces*, 2024, **16**, 31480-31488.
15. Z. Wu, Y. Feng, Z. Qin, X. Han, X. Zheng, Y. Deng and W. Hu, *Small*, 2022, **18**, 2106904.
16. J. Liu, J. Zhou and M. K. H. Leung, *ACS Appl. Mater. Interfaces*, 2022, **14**, 4399-4408.
17. Q. Cao, Z. Cheng, J. Dai, T. Sun, G. Li, L. Zhao, J. Yu, W. Zhou and J. Lin, *Small*, 2022, **18**, 2204827.